

Gas Transport Properties of 6FDA-Durene/1,3-Phenylenediamine (mPDA) Copolyimides

TAI-SHUNG CHUNG,^{1,2} WEN-HUI LIN,¹ ROHIT H. VORA²

¹ Department of Chemical Engineering, National University of Singapore, 10 Kent Ridge Crescent, Singapore 119260

² Institute of Materials Research and Engineering, 10 Kent Ridge Crescent, Singapore 119260

Received 15 August 2000; accepted 27 January 2001

ABSTRACT: The gas transport properties of He, H₂, O₂, N₂, and CO₂ for 6FDA-durene, 6FDA-mPDA, and their copolyimides have been investigated as a function of the composition, pressure, and temperature. The permeabilities, diffusion coefficients, and solubility coefficients follow the simple additional rules and Arrhenius relationships for 6FDA-durene/mPDA polyimides. The permeability decreases with an increase in pressure except He, and in the kinetic diameters of the penetrant molecules with the order of He, CO₂, O₂, and N₂. The diffusion coefficients of O₂, N₂, and CO₂ increase with increasing pressure and temperature. Interestingly, for these polyimides, the diffusion coefficient of O₂ is larger than that of CO₂. This may be caused by the strong quadrupole moment of the CO₂ molecules or the difficulty in estimating the accurate diameter of CO₂ molecules. The solubility coefficients decrease in the order of inherent condensability of the penetrant gases, namely CO₂, O₂, and N₂. In addition, WAXD results show that 6FDA-durene/mPDA polyimides are amorphous. The presence of a single glass transition temperature for these copolyimides indicates that these polyimides can be assumed to be random copolymers. They have excellent thermal stability exhibiting degradation temperature in a range of 493 to 548°C. © 2001 John Wiley & Sons, Inc. *J Appl Polym Sci* 81: 3552–3564, 2001

Key words: 6FDA-based polyimide; copolyimides; permeability; gas transport properties; fluoro-polyimides

INTRODUCTION

Polyimides have attracted much attention for separation membranes,^{1–6} especially for gas separation membranes, because some of them possess surprisingly high gas selectivities for gas pairs such as O₂/N₂ and CO₂/CH₄, as well as excellent spinnability, thermal stability, and mechanical strength. However, there still exists a tradeoff

relationship between gas permeability and permselectivity for polyimide membranes. To optimize polyimide materials for gas separation membranes, many works have been done on the structure property relationships of polyimides by systematically changing the diamine or dianhydride moieties.^{7–10} Among these studies, an empirical principle has been developed to tailor chemical structure to achieve high permeability and permselectivity. Bulky groups have been incorporated into the polymer backbone to inhibit intersegmental packing, leading to create pathways for gas diffusion or space for gas sorption, and often resulting in an increase in permeability, whereas rigid polymeric segments that restrict mobile

Correspondence to: T.-S. Chung; e-mail: chenctc@nus.edu.sg.
Contract grant sponsor: National University of Singapore;
contract grant number: RP960609A.

Journal of Applied Polymer Science, Vol. 81, 3552–3564 (2001)
© 2001 John Wiley & Sons, Inc.

linkages in the polymer backbones tend to enhance gas permselectivity.¹¹ The introduction of $-\text{C}(\text{CF}_3)_2-$ linkages into 6FDA (2,2'-bis (3,4'-dicarboxyphenyl) hexafluoropropane diandrydride)-based polyimides is a typical example. The $-\text{C}(\text{CF}_3)_2-$ linkages hinder the rotation of neighboring phenyl rings and enhance the permselectivity. As a result, some of 6FDA-based polyimides consistently deviate from the general tradeoff relationship between permeability and permselectivity by showing higher selectivities at values of permeability equivalent to other polymers.^{1,9,10}

Copolymerization is one of the approaches to develop new polymeric membranes for gas separations. It may combine the advantages of the base polymers and eliminate their deficiencies. In terms of gas permeability, copolymers generally exhibit a linear relationship between the log of permeability and the volume fraction of a specific monomer composition.¹² However, our previous work showed that some of 6FDA-durene/1,4-phenylenediamine (pPDA) copolyimides exhibited a positive deviation in gas permeability from the additional rule of the semilogarithmic equation. This interesting phenomenon was mainly attributed to higher solubility coefficients resulting from the generation of excess free volume in copolyimides.¹³ The observation prompts us to further investigate copolymerization effects on gas permeability of similar polyimides with different isomers. The objective of this work is, therefore, to study gas separation performance of the copolyimides synthesized from 2,2'-bis (3,4'-dicarboxyphenyl) hexafluoropropane diandrydride (6FDA), 2,3,5,6-tetramethyl-1,4-phenylenediamine (durene diamine), and 1,3-phenylenediamine (mPDA) with a dianhydride to diamine molar ratio of 1 : 1. The copolyimides consist of various fractions of two dis-

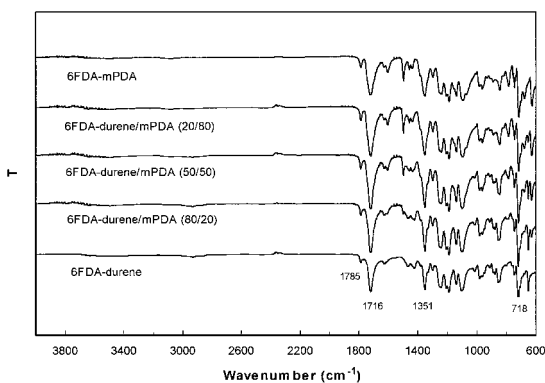


Figure 1 FTIR spectra of 6FDA-durene/mPDA (co)polyimides .

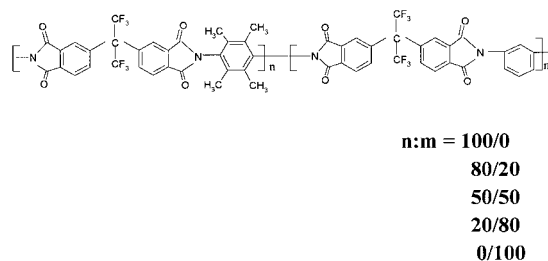


Figure 2 Chemical structures of 6FDA-durene/mPDA (co)polyimides.

tinct diamines—durene diamine and mPDA—which possess bulky and flat groups, respectively.

EXPERIMENTAL

Materials

The homo- and copolyimides studied in this work were prepared from 2,2'-bis (3,4'-dicarboxyphenyl) hexafluoropropane diandrydride (6FDA), 2,3,5,6-tetramethyl-1,4-phenylenediamine (durene diamine), and 1,3-phenylenediamine (mPDA) by the method reported elsewhere.^{14,15} Figure 1 shows the FTIR spectra for the 6FDA-durene/mPDA polyimides, which were determined by a Perkin-Elmer Spectrum 2000 FTIR spectrometer. The appearance of the absorption bands at 1785 cm^{-1} (symmetric stretch of the carbonyl group in the five-member ring), 1351 cm^{-1} (C—N stretch), and 718 cm^{-1} (deformation of the imide ring or to the imide carbonyl group) confirmed the formation of imides. There are no absorption bands at 3350 and 3180 cm^{-1} , 3320 – 3070 cm^{-1} , and 1670 – 1630 cm^{-1} , which were attributed to the amids and acids. This indicates that polyamic acids were completely converted to polyimides. The chemical structures of these polyimides are illustrated in Figure 2.

Methylene chloride of analytical reagent grade was purchased from BDH Laboratory Supplies (England) and used as received. Helium, hydrogen, oxygen, nitrogen, and carbon dioxide were obtained from SOXAL. The purity of CO_2 and O_2 is 99.8%, and the others are 99.995%. All the gases were used without further purification.

Preparation of Dense Flat Membranes

Dense films were prepared by casting a methylene chloride solution containing about 2 wt % polymer on clean leveled glass plates. After being dried at room temperature for 2 days, the films

were program thermally dried with specific heating rates, and finally vacuum dried at 250°C for 24 h. More details about the sample preparation have been reported in our previous article.¹³

Thermal and Physical Characterization

Molecular weight (M_w and M_n) of 6FDA-durene, 6FDA-mPDA, and their copolyimides were measured using a Gel Permeation Chromatography (GPC) (Waters 2690), with tetrahydrofuran (THF) as the carrier solvent and poly(styrene) as the standard. Film density was determined using a top-loading electronic Mettler Toledo balance with a density kit according to the Archimedean principle and by weighing samples in air and ethanol at room temperature. Wide-angle X-ray scattering (WAXS) measurements for the films were performed on an X'pert philips XRD with $\text{CuK}\alpha$ radiation (λ ; = 1.54 Å) at 45 kV and 40 mA. The angular range was 5–50°.

The glass transition temperatures were determined using a Perkin-Elmer Pyris 1 differential scanning calorimeter with a heating rate of 20°C/min. Thermogravimetric analysis (TGA) was conducted using a Perkin-Elmer TGA 7 to analyze their thermal stability. Under air atmosphere, the polymers were heated from 50 to 900°C at 20°C/min.

Pure Gas Permeability Measurement

Pure gas permeability coefficients for He, H₂, O₂, N₂, and CO₂ gases were measured by a constant volume-variable pressure method. Detail experimental procedure was described in the previous article.¹³ The gas permeability coefficient was calculated from the slope of the curve of the pressure on the permeation side vs. time (dp/dt), which was recorded by a computer with a data shuttle (workbench PC for windows-V5.01.14) at a steady state using the following equation:

$$P = \frac{273 \times 10^{10}}{760} \frac{VL}{AT \left(\frac{p_0 \times 76}{14.7} \right)} \frac{dp}{dt} \quad (1)$$

where P is the permeability coefficient of a membrane to gas i (1 barrer = 1×10^{-10} cm³ (STP)-cm/cm²-s-cm Hg); V is the volume of the downstream chamber (cm³); A is the effective area of the film (cm²), L is the thickness of the membrane (cm), P_0 is the pressure of the penetrant gas in the upstream chamber (psia); T is the absolute tem-

perature of the measurement (K), and dp/dt is the rate of pressure measured by the pressure sensor in the low-pressure downstream chamber (mmHg/s).

Apparent diffusion coefficients were estimated from the time lag (θ) by the following relationship:

$$D_{\text{app}} = \frac{L^2}{6\theta} \quad (2)$$

where L is the film thickness and θ is the time lag.

Apparent solubility coefficient S may be evaluated from the relationship

$$S_{\text{app}} = P/D \quad (3)$$

Ideal permselectivity of a membrane for gas A to gas B was calculated from

$$\alpha_{A/B} = P_A/P_B \quad (4)$$

RESULTS AND DISCUSSION

Physical and Thermal Properties

WAXD curves of all polyimides were broad and without obvious peak features, indicating that homo- and copolyimides synthesized from 6FDA, durene, and mPDA were all amorphous. Table I lists the physical properties of the homo- and copolyimides. Fractional free volume calculations, which utilize experimentally measured densities, provide an alternative method for analyzing the degree of chain packing. The fractional free volume is defined as the specific free volume divided by the occupied volume. The specific free volume, $V_f = (V - V_0)$, is defined as the difference between the observed specific volume, V , and the occupied volume V_0 . The observed specific volume, V , is calculated from the measured density and the occupied volume, V_0 , is calculated from the correlation, $V_0 = 1.3V_w$, where V_w is the Van der Waals volume, which is estimated using the Bondi's group contribution method for homopolyimides.¹⁶ For the copolyimides, V_w is estimated by the equation $V_w = m_1V_{w1} + m_2V_{w2}$, where m_1 and m_2 are the molar fractions, V_{w1} and V_{w2} are the Van der Waals volume of homopolymers 1 and 2, respectively. It can be seen that fractional free volume decreases with increasing 6FDA-mPDA content in the copolyimides.

Degradation temperature can be used to present the thermal stability of a polymer in an

Table I Physical Properties of 6FDA-Durene/mPDA (co)polyimides

Polymer	η_{inh} dL/g	M_n	M_w	T_g °C	T_d °C	ρ g/cm ³	FFV
6F-durene	1.00	90,000	143,000	424	496	1.333	0.180
6F-durene/mPDA (80/20)	1.23	105,017	299,419	399	500	1.356	0.176
6F-durene/mPDA (50/50)	0.84	69,933	176,815	378	515	1.385	0.177
6F-durene/mPDA (20/80)	1.01	88,495	285,287	319	534	1.426	0.173
6F-mPDA	0.84	76,171	192,545	301	548	1.472	0.160

η_{inh} : intrinsic viscosity in NMP.

T_d : degradation temperature at 5 wt % loss in air.

T_g : glass transition temperatures calculated by the half C_p extrapolated method.

air atmosphere. When defined the degradation temperature as the temperature where 5 wt % loss is achieved, these 6FDA-durene/mPDA homo- and copolymers exhibit degradation temperatures in a range of 493 to 548°C. The thermal stability increases with increasing mPDA fraction in the polymer backbone.

As shown in Table I, the glass transition temperature of 6FDA-durene is higher than that of 6FDA-mPDA. Compared with the structure of 6FDA-mPDA, 6FDA-durene has four methyl substitutions on the phenyl ring in the diamine moiety, which hinder the phenyl ring rotation and result in an increase in chain stiffness. The T_g of the 6FDA-durene/mPDA copolyimides decrease with an increase in mPDA content, and the presence of a single glass transition temperature indicates that there is no phase separation in these materials, which are assumed to be random copolymers. For the readers' information, T_g of 6FDA-mPDA ($T_g = 301^\circ\text{C}$) is much lower than that of 6FDA-pPDA ($T_g = 350^\circ\text{C}$).¹³ This indi-

cates that *p*-phenylene linkages inhibit chain mobility greater than that of *m*-phenylene; thus, the latter may have more efficient chain packing than the former, which is consistent with the previous reports.^{17,18}

For random copolymers, the Fox equation¹⁹ can be utilized to predict the glass transition temperature, T_g , of a copolymer composed of two types of monomer sequence units (i.e., 6FDA-durene and 6FDA-mPDA) as follows:

$$\frac{1}{T_g} = \frac{w_1}{T_{g1}} + \frac{w_2}{T_{g2}} \quad (5)$$

where w_1 and w_2 are the weight fractions, and T_{g1} and T_{g2} (K) are the glass transition temperatures of homopolymers 1 and 2, respectively. The weight fraction was defined as the following equation:

$$w_1 = \frac{m_1 M_1}{m_1 M_1 + m_2 M_2} \quad (6)$$

Table II Glass Transition Temperature as a Function of 6FDA-Durene Content for 6FDA-Durene/mPDA (co)polyimides

Polymer	T_g (°C)	T_g (°C) Calculated from the Fox Equation	ΔT_g (°C)
6FDA-durene	424		
6FDA-durene/mPDA (80/20) ^a	399	398	1
6FDA-durene/mPDA (50/50) ^a	378	360	18
6FDA-durene/mPDA (20/80) ^a	319	324	-5
6FDA-mPDA	301		
6FDA-durene/pPDA (80/20) ^a	422	409	13
6FDA-durene/pPDA (50/50) ^a	406	387	19
6FDA-durene/pPDA (20/80) ^a	397	365	32
6FDA-pPDA	350		

^a In a molar ratio of diamines in a diamine mixture.

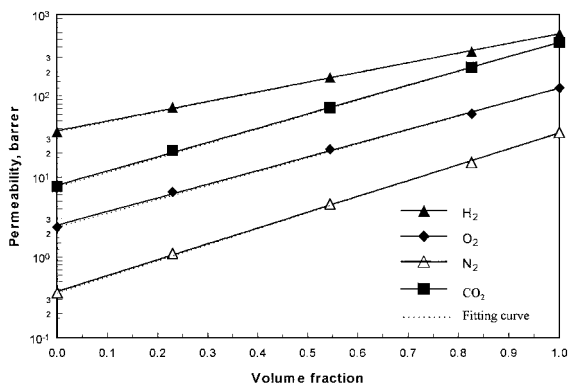


Figure 3 Effect of the volume fraction of the 6FDA-durene component on permeability coefficients for 6FDA-durene/mPDA (co)polyimide membranes.

where m_1 and m_2 are the molar fractions, and M_1 and M_2 are the molecular weights per mol of homopolymers 1 and 2. Here molecular weights of 6FDA-durene and 6FDA-mPDA are 572.43 and 516.34 g/mol, respectively.

Table II summarizes a comparison between the predicted T_g and experimental data for 6FDA-durene/mPDA copolyimides. The results calculated from the Fox equation are in good agreement with the experimental data except for 6FDA-durene/mPDA (50/50). For comparison, T_g s of 6FDA-durene/pPDA copolyimides are much higher than those calculated from the equation, as listed in Table II. This suggests that the conformation differences between 6FDA-durene and 6FDA-mPDA are much less than those between 6FDA-durene and 6FDA-pPDA.

The Effect of Composition on Gas Transport Properties

Figure 3 illustrates the semilogarithmic plot of H_2 , O_2 , N_2 , and CO_2 permeabilities of 6FDA-du-

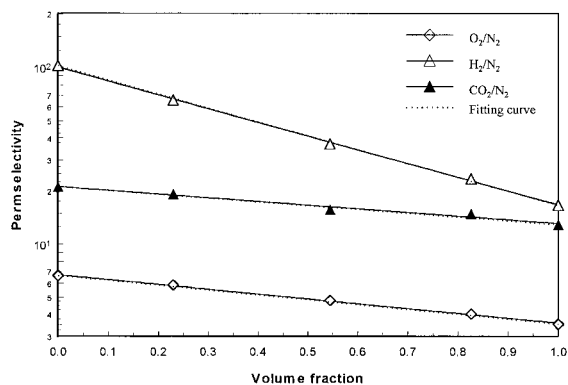


Figure 4 Effect of volume fraction of 6FDA-durene component on permselectivity for 6FDA-durene/mPDA (co)polyimide membranes.

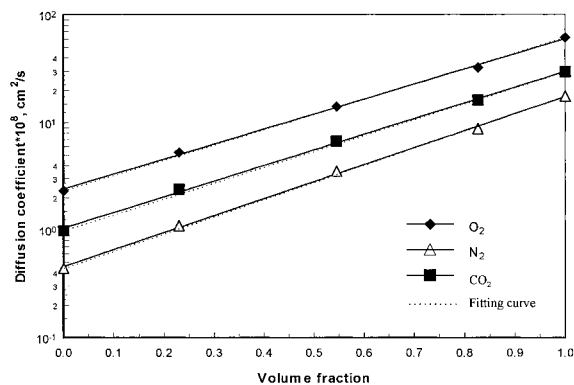


Figure 5 Effect of volume fraction of the 6FDA-durene component on diffusion coefficients for 6FDA-durene/mPDA (co)polyimide membranes.

rene, 6FDA-mPDA, and 6FDA-durene/mPDA copolyimides determined from pure gas measurements vs. the volume fraction of the 6FDA-durene component in 6FDA-durene/mPDA copolyimides. The gas permeability measurements for these materials were carried out at 10 atm except H_2 at 3.5 atm. As shown in Figure 3, the permeability of each gas increases linearly with an increase in 6FDA-durene content in the copolyimides. In other words, the relationship between permeability and monomer composition for these copolyimides is in accord with the simple additional rule suggested by Barnabeo et al.,¹² which can be expressed as follows:

$$\ln P = \phi_1 \ln P_1 + \phi_2 \ln P_2 \quad (7)$$

where ϕ is the volume fraction, P is the permeability, and 1 and 2 subscribes refer to the two homopolymers. The permeability decreases ac-

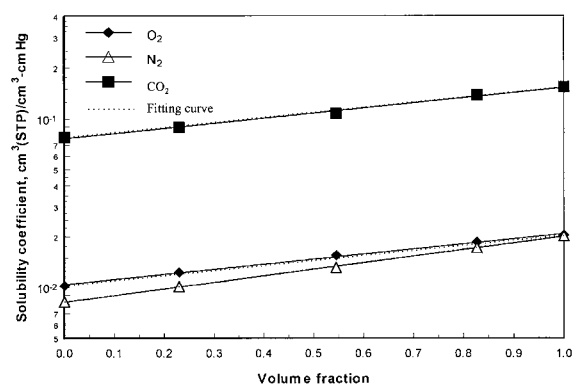


Figure 6 Effect of volume fraction of the 6FDA-durene component on solubility coefficients for 6FDA-durene/mPDA (co)polyimide membranes.

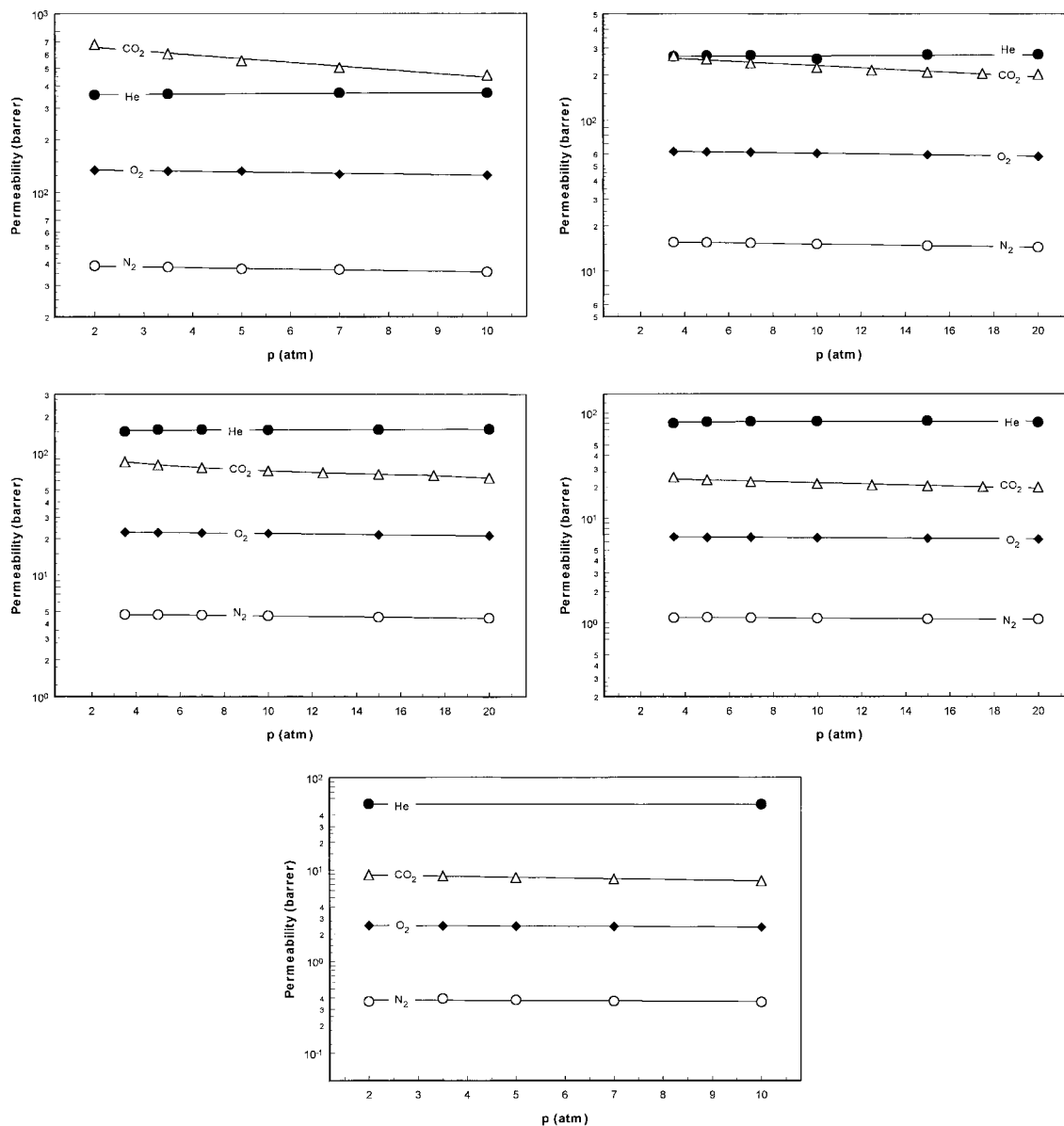


Figure 7 (a) Gas permeability as a function of feed pressure for 6FDA-durene dense membranes at 35°C. (b) Gas permeability as a function of feed pressure for 6FDA-durene/mPDA(80/20) dense membranes at 35°C. (c) Gas permeability as a function of feed pressure for 6FDA-durene/mPDA (50/50) dense membranes at 35°C. (d) Gas permeability as a function of feed pressure for 6FDA-durene/mPDA (20/80) dense membranes at 35°C. (e) Gas permeability as a function of feed pressure for 6FDA-mPDA dense membranes at 35°C.

According to this order: H₂ (kinetic diameter of 2.89 Å) > CO₂ (3.30 Å) > O₂ (3.46 Å) > N₂ (3.64 Å). This order follows exactly the same order of increasing “kinetic” diameters of the penetrant molecules. Figure 4 suggests that the gas permselectivities of ($P_{\text{CO}_2}/P_{\text{N}_2}$), ($P_{\text{O}_2}/P_{\text{N}_2}$), and ($P_{\text{H}_2}/P_{\text{N}_2}$) also follow the simple additional rule for these copolyimides.

Permeability is a function of diffusion coefficient and solubility coefficient. To understand the permeability variation, it is necessary to investigate the effects of durene content in the copolyimides on diffusivity and solubility. Figure 5 illustrates the apparent gas diffusion coefficients of various gases for 6FDA copolyimide membranes as a function of the 6FDA-durene volume fraction.

Table III Pressure Dependence

Pressure atm	$D \times 10^8, \text{cm}^2/\text{s}$			D_A/D_B	
	O ₂	N ₂	CO ₂	O ₂ /N ₂	CO ₂ /N ₂
(a) of 6FDA-durene/mPDA (80/20) diffusion coefficients at 35°C					
3.5	30.99	8.72	12.09	3.55	1.39
5.0	31.27	8.76	12.98	3.57	1.48
7.0	31.09	8.75	14.58	3.55	1.67
10.0	32.47	8.75	16.19	3.71	1.85
12.5	—	—	17.63	—	—
15.0	33.82	9.24	18.88	3.66	2.04
17.5	—	—	19.90	—	—
20.0	35.13	9.70	20.93	3.62	2.16
(b) of 6FDA-durene/mPDA (50/50) diffusion coefficients at 35°C					
3.5	12.92	3.48	4.77	3.72	1.37
5.0	13.34	3.50	5.30	3.81	1.51
7.0	13.76	3.50	5.90	3.93	1.68
10.0	14.12	3.51	6.70	4.03	1.91
12.5	—	—	7.35	—	—
15.0	14.81	3.66	7.91	4.05	2.16
17.5	—	—	8.47	—	—
20.0	15.57	3.90	9.13	3.99	2.34
(c) of 6FDA-durene/mPDA (20/80) diffusion coefficients at 35°C					
3.5	4.95	0.99	1.72	4.98	1.73
5.0	5.10	1.04	1.88	4.92	1.81
7.0	5.11	1.06	2.10	4.80	1.98
10.0	5.28	1.09	2.39	4.82	2.19
12.5	—	—	2.61	—	—
15.0	5.42	1.16	2.82	4.69	2.43
17.5	—	—	3.00	—	—
20.0	5.75	1.22	3.19	4.72	2.62
(d) of 6FDA-mPDA diffusion coefficients at 35°C					
2.0	2.068	0.392	0.552	5.28	1.41
3.5	2.103	0.428	0.651	4.92	1.52
5.0	2.201	0.430	0.743	5.12	1.73
7.0	2.213	0.422	0.843	5.25	2.00
10.0	2.322	0.436	0.976	5.33	2.24
12.5	—	—	1.096	—	—
15.0	—	—	1.146	—	—
17.5	—	—	1.227	—	—
20.0	—	—	1.307	—	—

The dashed lines in Figure 5 are the gas diffusion coefficients (D) calculated from the rule of semi-logarithmic addition as follows:^{12,20}

$$\ln D = \phi_1 \ln D_1 + \phi_2 \ln D_2 \quad (8)$$

where ϕ is the volume fraction, D_i is the apparent diffusion coefficient, and 1 and 2 subscribes refer

to the two homopolymers. It can be seen that the diffusion coefficients of O₂, N₂, and CO₂ increase linearly with an increase in volume fraction of the 6FDA-durene content, indicating that the diffusivity for these copolyimides follows the additive rule. The trend of diffusivity decrease follows this order: O₂ (kinetic diameter of 3.46 Å) > CO₂ (3.30 Å) > N₂ (3.64 Å).²¹ Except CO₂, this decreasing

Table IV Pressure Dependence

Pressure atm	$S, \text{cm}^3(\text{STP})/\text{cm}^3\text{-cmHg}$			S_A/S_B	
	O_2	N_2	CO_2	O_2/N_2	CO_2/N_2
(a) of 6FDA-durene/mPDA (80/20) solubility coefficients at 35°C					
3.5	0.0201	0.0178	0.2217	1.13	12.46
5.0	0.0198	0.0177	0.1960	1.12	11.07
7.0	0.0197	0.0175	0.1637	1.13	9.35
10.0	0.0186	0.0172	0.1379	1.08	8.02
12.5	—	—	0.1213	—	—
15.0	0.0175	0.0159	0.1101	1.10	6.92
17.5	—	—	0.1025	—	—
20.0	0.0164	0.0148	0.0961	1.11	6.49
(b) of 6FDA-durene/mPDA (50/50) solubility coefficients at 35°C					
3.5	0.0174	0.0135	0.1784	1.29	13.21
5.0	0.0168	0.0134	0.1513	1.25	11.29
7.0	0.0161	0.0133	0.1292	1.21	9.71
10.0	0.0155	0.0131	0.1072	1.18	8.18
12.5	—	—	0.0943	—	—
15.0	0.0145	0.0123	0.0851	1.18	6.92
17.5	—	—	0.0777	—	—
20.0	0.0135	0.0113	0.0686	1.19	6.07
(c) of 6FDA-durene/mPDA (20/80) solubility coefficients at 35°C					
3.5	0.0134	0.0113	0.1427	1.19	12.63
5.0	0.0129	0.0109	0.1237	1.18	11.35
7.0	0.0128	0.0105	0.1059	1.22	10.09
10.0	0.0123	0.0101	0.0890	1.22	8.81
12.5	—	—	0.0792	—	—
15.0	0.0119	0.0094	0.0721	1.27	7.67
17.5	—	—	0.0665	—	—
20.0	0.0110	0.0089	0.0620	1.24	6.97
(d) of 6FDA-mPDA solubility coefficients at 35°C					
2.0	0.0119	0.0093	0.1593	1.28	17.13
3.5	0.0117	0.0091	0.1310	1.29	14.40
5.0	0.0110	0.0087	0.1106	1.26	12.71
7.0	0.0108	0.0087	0.0938	1.24	10.78
10.0	0.0102	0.0082	0.0775	1.24	9.45
12.5	—	—	0.0663	—	—
15.0	—	—	0.0626	—	—
17.5	—	—	0.0571	—	—
20.0	—	—	0.0530	—	—

trend with the penetrant diameter is the same as that of permeability coefficients. Interestingly, for all the polyimides studied in the work, $D(\text{O}_2) > D(\text{CO}_2)$, whereas $P(\text{CO}_2) > P(\text{O}_2)$. The surprisingly large diffusion coefficient of O_2 relative to CO_2 is not consistent with the “kinetic” molecular diameters of O_2 and CO_2 , because $\sigma_K(\text{O}_2)$

$> \sigma_K(\text{CO}_2)$. In most cases, diffusion coefficients of gases in glassy polymers decrease as the kinetic diameter of the penetrant molecule increases. A similar behavior has been reported for other polymers.^{7,22,23} A possible cause for the lower diffusion coefficients of CO_2 compared to those of O_2 is the strong quadrupole moment of CO_2 molecules

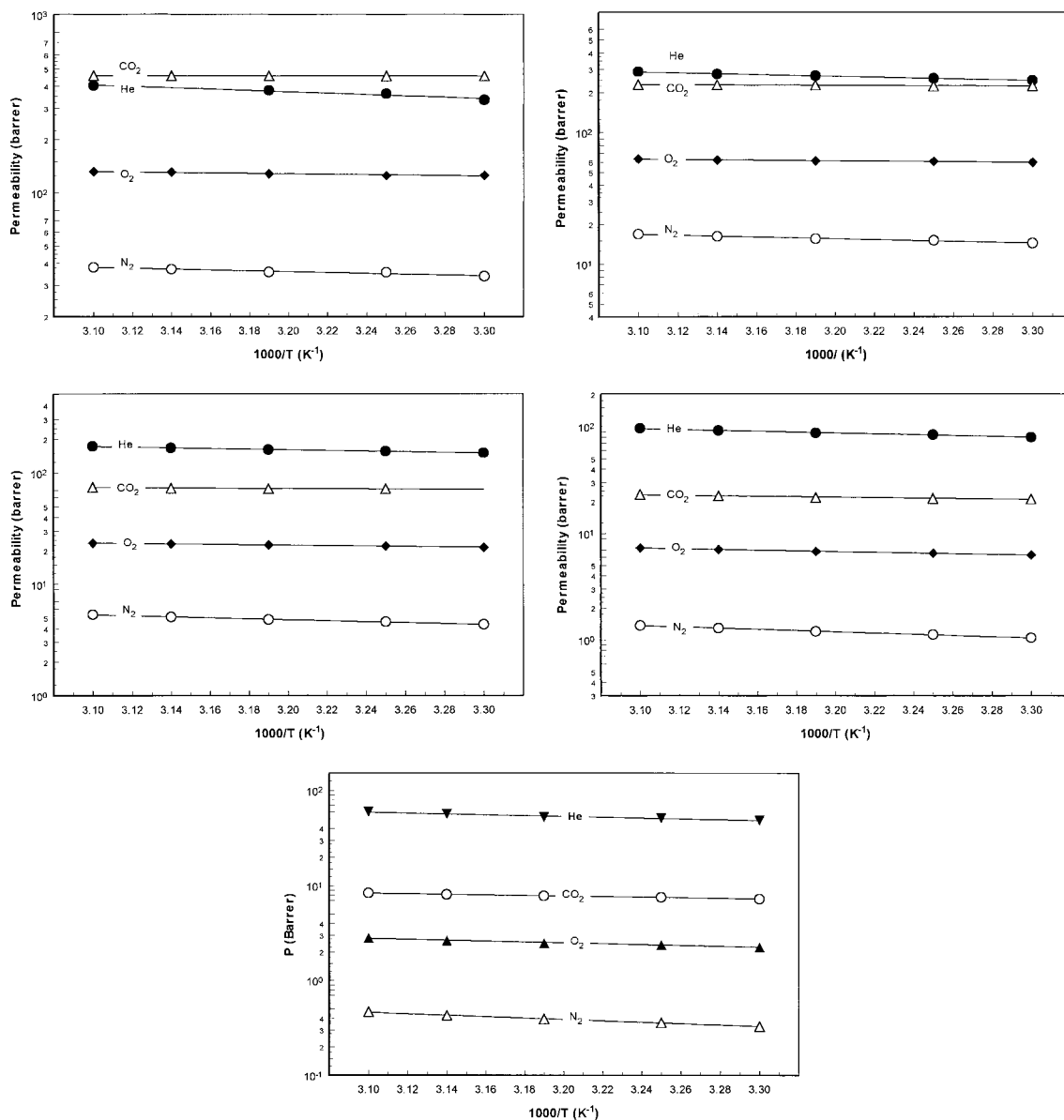


Figure 8 (a) Temperature dependence of 6FDA-durene permeabilities at 10 atm. (b) Temperature dependence of 6FDA-durene/mPDA (80/20) permeabilities at 10 atm. (c) Temperature dependence of 6FDA-durene/mPDA (50/50) permeabilities at 10 atm. (d) Temperature dependence of 6FDA-durene/mPDA (20/80) permeabilities at 10 atm. (e) Temperature dependence of 6FDA-mPDA permeabilities at 10 atm.

$(4.1 \times 10^{-26} \text{ esu.cm}^2)$, which may result in specific interactions between CO_2 and the polar groups in the 6FDA polyimides, for example, the $-(\text{CF}_3)_2-$ and $\text{C}=\text{O}$ groups in their dianhydride moieties. The interactions may hinder the mobility of CO_2 molecules in the polyimide matrix.⁶

Figure 6 shows that O_2 , N_2 , and CO_2 solubility coefficients increase with an increase in volume fraction of the 6FDA-durene content and follow the additive rule. The solubility coefficients of O_2 ,

N_2 , and CO_2 in these polyimides decrease in the order of $\text{CO}_2 > \text{O}_2 > \text{N}_2$, which is consistent with the decreasing order of inherent condensability of these gases. CO_2 possesses higher inherent condensability, resulting in a greater solubility coefficient. In addition, the solubility selectivity for gas pair CO_2/N_2 in all polyimides studied is much higher than its corresponding diffusivity selectivity, and the overall selectivity for gas pair CO_2/N_2 is mainly determined by the high solubility selec-

Table V Activation Energy of Various Gases for Permeation of 6FDA-durene/mPDA (co)polyimides Dense Membranes at 10 atm

Polymer	E_p (kJ/mol)			
	He	O ₂	N ₂	CO ₂
6FDA-durene	7.38	2.40	4.45	0.20
6FDA-durene/mPDA (80/20)	6.34	2.41	6.45	1.18
6FDA-durene/mPDA (50/50)	5.68	3.81	8.36	1.85
6FDA-durene/mPDA (20/80)	7.36	6.20	11.03	3.92
6FDA-mPDA	8.29	9.01	14.53	5.86

tivity like most of polymeric membranes. In contrast, the diffusivity selectivity for gas pairs O₂/N₂ is higher than their corresponding solubility selectivity. Thus, high O₂/N₂ permselectivities mainly result from their high diffusion selectivity.

The Effect of Pressure on Gas Separation Performance

Figure 7(a)–(e) exhibits the permeabilities of He, O₂, N₂, and CO₂ as a function of upstream pressure for 6FDA-durene, 6FDA-mPDA, and their copolyimides dense flat membranes at 35°C. The permeability of He slightly increases, while the permeabilities of O₂, N₂, and CO₂ decrease with an increase in the upstream pressure. The largest permeability decrease with increasing pressure is observed with CO₂, the most condensable species of the six gases. No CO₂-induced plasticization is noticed in this testing pressure range. The pressure dependence of permeability is consistent with the dual-mode transport model used to describe the gas transport behavior of glassy polymers, which is represented as the sum of the Henry mode and the Langmuir mode as follows:^{24,25}

$$P = k_D D_D + C'_H D_H b / (1 + bp) \quad (9)$$

where P is the permeability, k_D is the solubility coefficient for Henry's law, C'_H is the Langmuir capacity constant, b is the affinity constant, D_D and D_H are the diffusion coefficients for Henry's law and Langmuir mode, respectively, and p is the upstream gas pressure (downstream pressure is approximately zero). In general, the Langmuir mode, which is associated with the "excess" free volume formed in the glassy state, makes a large contribution to the nature of pressure dependence

of the permeability in a glassy polymer. For He, its solubility coefficient is very small; thus, the Langmuir mode sorption does not play an important role to affect the permeability. The pressure dependence of diffusion coefficient governs the permeation process, leading to a small increase in He permeability as a function of the upstream pressure.

Table III(a–d) summarizes the apparent diffusion coefficients change as a function of pressure, while Table 4(a–b) tabulates the calculated apparent solubility coefficients various with pressure. The diffusion coefficients of O₂, N₂, and CO₂ increase with increasing pressure, whereas the corresponding solubility coefficients decrease with an increase in pressure. This behavior can be explained using the dual-mode sorption and partial immobilisation theory developed by Koros and Paul.^{24,25} For most glassy polymers at low-pressure environments, gas molecules are sorbed into Langmuir mode sites (intersegmental packing defects) more easily than into Henry's mode sites. The situation changes at high-pressure environments. Henry's mode sorption becomes predominant because of the easy saturation of Langmuir sites. Because gases sorbed into Henry's sites have greater diffusivity than those into Langmuir sites, gas diffusivity at low pressures is relatively low because most diffusion occurs in the Langmuir sites. The apparent diffusivity increases, and reaches the asymptotic limit of the diffusivity of Henry's Law proportion at high pressures.

The permselectivity of O₂/N₂ is almost constant, and the permselectivity of CO₂/N₂ decreases with increasing pressure. For 6FDA-durene/mPDA films, the decrease in the solubility selectivity governs the process. Thus, this opposite effect causes the permeability selectivity decreases with increasing pressure.

The Effect of Temperature on the Gas Transport Property

The temperature dependence of He, O₂, N₂, and CO₂ permeabilities for 6FDA-durene, 6FDA-mPDA, and 6FDA-durene/mPDA copolyimides were determined at 10 atm upstream pressure, and the results are presented in Figure 8(a)–(e). The permeation coefficients are shown to be a function of the reciprocal temperature, as expressed by the Arrhenius relationship:²⁶

$$P = P_0 \exp\left(\frac{-E_p}{RT}\right) \quad (10)$$

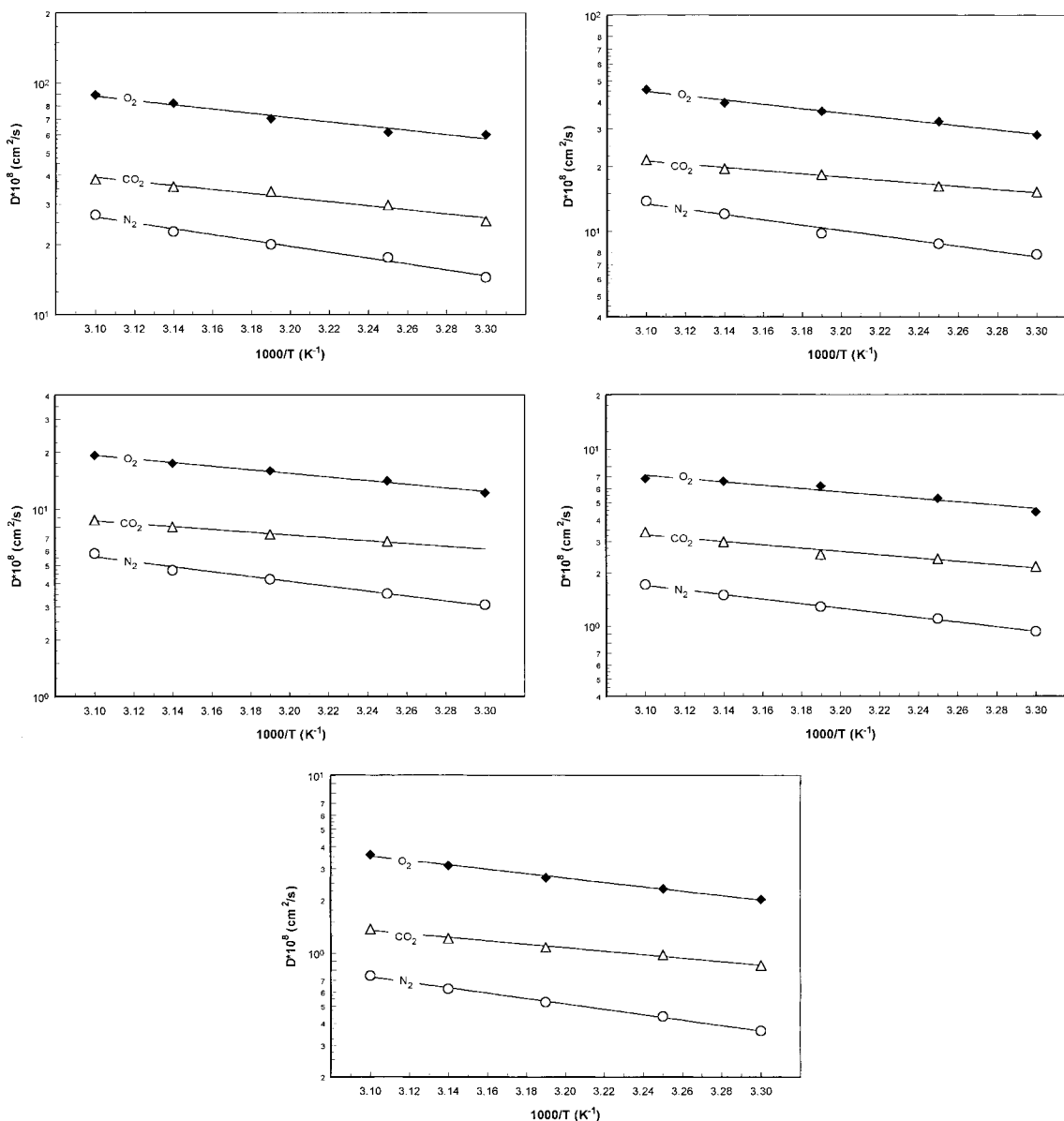


Figure 9 (a) Temperature dependence of diffusion coefficients for 6FDA-durene dense membranes at 10 atm. (b) Temperature dependence of diffusion coefficients for 6FDA-durene/mPDA (80/20) dense membranes at 10 atm. (c) Temperature dependence of diffusion coefficients for 6FDA-durene/mPDA (50/50) dense membranes at 10 atm. (d) Temperature dependence of diffusion coefficients for 6FDA-durene/mPDA (20/80) dense membranes at 10 atm. (e) Temperature dependence of diffusion coefficients for 6FDA-mPDA dense membranes at 10 atm.

Where P_0 is a preexponential factor, E_p the activation energy for permeation, R the universal gas constant, and T the absolute temperature. The permeability coefficients increase with temperature for all the tested gases. The temperature dependence of permeability is a combination of the temperature dependencies of diffusion and sorption. In general, the diffusion coefficient in-

creases with temperature, while the sorption coefficient decreases. These two aspects exhibit opposite effects on the permeation, but the relative change in diffusion coefficient is usually greater than that in sorption coefficient.

Table V summarizes the calculated activation energies of O₂, N₂, and CO₂ for permeation and the corresponding preexponential factors for

Table VI Activation Energy of Various Gases for Diffusion of 6FDA-durene/mPDA (co)polyimide Dense Membranes at 10 atm

Polymer	E_d (kJ/mol)		
	O ₂	N ₂	CO ₂
6F-durene	17.55	24.29	16.80
6FDA-durene/mPDA (80/20)	18.89	23.49	14.11
6FDA-durene/mPDA (50/50)	18.44	25.22	14.63
6FDA-durene/mPDA (20/80)	18.02	24.95	18.08
6FDA-mPDA	23.63	29.31	18.86

these copolyimides obtained from the Arrhenius plots. With the exception of He, the activation energies for O₂, N₂, and CO₂ increase with increasing 6FDA-mPDA content in the copolyimides because of the increase in chain rigidity. In addition, E_p increases with increasing molecular size of the penetrant gas, following the order of CO₂, O₂, and N₂.

Although permeability coefficients increase with temperature, permselectivities for important gas pairs (O₂/N₂, and CO₂/N₂) decrease due to differences in activation energies of permeation for various gases. Quantitatively, a negative $\Delta E_{p,A,B}$ between A and B penetrants indicates a decrease in permselectivity with increasing temperature. For these polyimides, temperature dependence of CO₂/N₂ permselectivity is much larger than that of O₂/N₂ pair.

Figure 9(a)–(e) show that diffusion coefficients of all gases increase with increasing temperature because of greater interstice among polymeric chains and additional larger scale chain motion at elevated temperatures. The activation energy for diffusion increases with increasing gas molecular size and 6FDA-mPDA content, as presented in Table VI. Although the diffusion coefficient of O₂ is larger than that of CO₂, the activation energy for O₂ diffusion is greater than that of CO₂. This interesting phenomenon seems to be contradictory to our instinct prediction that the activation energy for O₂ diffusion should be smaller than that of CO₂, indicating that a gas possessing higher activation energy for diffusion may not lead to a lower diffusion coefficient.

CONCLUSION

The gas transport properties of 6FDA-durene and 6FDA-mPDA homopolymers and their copolyim-

ides have been determined as a function of pressure and temperature. It is found that the semi-logarithmic plot of H₂, O₂, N₂, and CO₂ permeabilities increase linearly with an increase in volume fraction of the 6FDA-durene component in these polyimides. The permeabilities of these polyimides decrease with increasing “kinetic” diameter of the penetrant gas with the following order: H₂ > CO₂ > O₂ > N₂. Interestingly, for all the polyimides studied, the diffusivity of O₂ is great than that of CO₂ even though the permeability of latter is lower than the former. This may be caused by the strong quadruple moment of the CO₂ molecules or the difficulty in estimating the accurate diameter of CO₂ molecules.

The solubility selectivity of CO₂/N₂ in these polyimides is much higher than the corresponding diffusivity selectivity, and the selectivity of CO₂/N₂ is mainly determined by the solubility selectivity. In contrast, the diffusivity selectivity of O₂/N₂ is higher than their solubility selectivities. The permselectivity of O₂/N₂ is mainly controlled by their diffusion selectivity.

An increase in the upstream pressure results in a slightly increase in He permeability and a decrease in O₂, N₂, and CO₂ permeabilities. The largest permeability decrease with increasing pressure is observed with CO₂, the most condensable gas in this study. The permeation coefficient follows the Arrhenius relationship. With the exception of He, the activation energies of O₂, N₂, and CO₂ increase with increasing gas molecular size and 6FDA-mPDA content in the copolyimides.

The authors would like to thank National University of Singapore (NUS) (Research Grant No: RP960609A) for funding this project. Thanks are due to Mr. S. L. Liu for his technical support in gas permeation measurements; Mr. K. P. Ng of the Department of Chemical and Environmental Engineering for his help in fabrication and machinery of permeation cells; and Dr. R. Wang's membrane team and the Institute of Materials Research and Engineering of Singapore for using their equipment and financial award. Special thanks are due to Professor D. R. Paul at U. of Texas for providing technical support for the permeation apparatus.

REFERENCES

1. Koros, W. J.; Fleming, G. K.; Jordan, S. M.; Kim, T. H.; Hoehn, H. H. *Prog Polym Sci* 1988, 13, 339.
2. Paul, D. R.; Yampol'skii Y.P., Eds. *Polymeric Gas Separation Membranes*; CRC Press: Boca Raton, FL, 1994.
3. Robeson, L. M. *J Membr Sci* 1991, 62, 165.

4. Robeson, L. M.; Smith, C. D.; Langsam, M. J. *J Membr Sci* 1997, 132, 33.
5. Chung, T. S.; Kafchinski, E. R.; Vora, R. *J Membr Sci* 1994, 88, 21.
6. Wang, W. Y.; Ugomori, T.; Tanaka, K.; Kita, H.; Okamoto, K.; Suma, Y. *J Polym Sci Polym Phys* 2000, 38, 2954.
7. Stern, S. A.; Liu, Y.; Feld, W. A. *J Polym Sci Polym Phys* 1993, 31, 939.
8. Mi, Y.; Stern, S. A.; Trohalaki, S. *J Membr Sci* 1993, 77, 41.
9. Hirayama, Y.; Yoshinaga, T.; Kusuki, Y.; Ni-nomiya, K.; Sakakibara, T.; Tamari, T. *J Membr Sci* 1996, 111, 169.
10. Semenova, S. I. In *Polyimide Membrane: Application, Fabrications, and Properties*; Ohya, H.; Kudryavtsev, V. V.; Semenova, S. I., Eds.; Gordon and Breach Publishers: Tokyo, 1996, p. 103, Chap 4.
11. Zimmerman, C. M.; Koros, W. J. *Polymer* 1999, 40, 5655.
12. Barnabeo, A. E.; Creasy, W. S.; Robeson, L. M. *J Polym Sci Polym Chem* 1975, 13, 1979.
13. Lin, W. H.; Vora, R. H.; Chung, T. S. *J Polym Sci Polym Phys* 2000, 38, 2703.
14. Vora, R. H. U.S. Pat. 4,933,132 (1990).
15. Vora, R. H.; Goh, S. H.; Chung, T. S. *Polym Eng Sci* 2000, 40, 1318.
16. Bondi, A.; *J Chem Phys* (van der Waals volume and radii) 1964, 68, 441.
17. Zoia, G.; Stern, S. A.; St. Clair, A. K.; Pratt, J. R. *J Polym Sci Polym Phys* 1994, 32, 53.
18. Coleman, M. R.; Koros, W. J. *J Membr Sci* 1990, 50, 285.
19. Fox, T. G. *Bull Am Phys Soc* 1956, 1, 123.
20. Paul, D. R. *J Membr Sci* 1984, 18, 75.
21. Breck, B. W. *Zeolite Molecular Sieves*; John Wiley & Sons: New York, 1974.
22. Zimmerman, C. M.; Koros, W. J. *J Polym Sci Polym Phys* 1999, 37, 1235.
23. Shieh, J. J.; Chung, T. S. *J Polym Sci Polym Phys* 1999, 37, 2851.
24. Koros, W. J.; Paul, D. R.; Rocha, A. A. *J Polym Sci Polym Phys* 1976, 14, 687.
25. Koros, W. J.; Paul, D. R. *J Polym Sci Polym Phys* 1978, 16, 2171.
26. Stannett, V. In *Diffusion in Polymers*; Crank, J.; Park, G. S., Eds.; Academic Press: New York, 1968, Chap 2.